JFE TECHNICAL REPORT
No. 23 (Mar. 2018)

Factors Affecting Surface Roughness of Low Carbon Resulfurized Free Cutting Steel†

IMANAMI Yuta[*1] TOMITA Kunikazu[*2] NISHIMURA Kimihiro[*3]

Abstract:

Factors affecting surface roughness after cutting low carbon resulfurized free cutting steel have been reported in many papers in the past. However, most of studies were carried out using high speed steel tools instead of cemented carbide or ceramics tools which are becoming more popular recently. In this study, effect of tool materials and steel factors such as sulfides and yield ratio on surface roughness after cutting was studied. As a result, difference of thermal conductivity among tool materials changes cutting temperature. Change in cutting temperature affects surface roughness through formation behavior of built-up edge. On the other hand, from the viewpoint of steel factors, enlarging sulfides, decreasing aspect ratio of sulfides and increasing yield ratio are effective in order to reduce surface roughness with both cemented carbide tools and ceramic tools.

1. Introduction

Lead-free low carbon resulfurized free cutting steel and low carbon resulfurized and leaded free cutting steel are frequently used in precision parts of OA equipment and similar products, and satisfactory surface roughness after cutting is required in product specifications. Because lead-free free cutting steels have been strongly demanded from the viewpoint of global environmental problems in recent years, it is important to improve the machinability of these materials. The various factors which can affect surface roughness after cutting are arranged in **Table 1**. Although many reports have discussed the relationship between these factors and the surface roughness of low carbon resulfurized free cutting steel, those researches[1)] were mainly carried out using high speed steel tools. However, tool of materials other than high speed steel, such as cemented carbide tools or ceramic tools, have become increasingly popular in recent years. Therefore, in this research, the effect of the type of tool material on surface roughness after cutting was studied. In addition, the influence of factors related to the free cutting steel on surface roughness after cutting was also investigated with tools of materials other than high speed steel.

Table 1 Factors on surface roughness after cutting

No.	Factors	No.	Factors
1	Cutting speed	5	Tool material
2	Feed rate	6	Lubricant
3	Insert nose radius	7	Rigidity of cutting machine
4	Rake angle	8	Worked material

2. Influence of Tool Material on Surface Roughness

2.1 Experimental Method

Table 2 shows the chemical compositions of the tested steels. As a low carbon resulfurized free cutting steel, JIS standard SUM23 was melted with actual equipment and hot-rolled to a round bar with a diameter of 110 mm. Vickers hardness (HV) was measured at a depth of 2 mm from the surface of the obtained round bar. After mirror polishing of the cross section, it was etched with a 3% Nital solution and observed with an optical microscope. For surface roughness, 10

† Originally published in *JFE GIHO* No. 39 (Feb. 2017), p. 43–48

[*1] Senior Researcher Deputy Manager,
Steel Bar & Wire Rod Research Dept.,
Steel Res. Lab.,
JFE Steel

[*2] Dr. Eng.,
Senior Researcher General Manager,
Steel Bar & Wire Rod Research Dept.,
Steel Res. Lab.,
JFE Steel

[*3] General Manager,
Steel Bar & Wire Rod Research Dept.,
Steel Res. Lab.,
JFE Steel

Table 2 Chemical compositions of steels (Mass%)

Steel	C	Si	Mn	P	S	Al
SUM23	0.08	−	1.2	0.07	0.33	−
S10C	0.08	0.2	0.4	0.02	0.01	0.024

Table 3 Turning test conditions

Tool shape	TNGN160404	Tool material	Cemented carbide: K10
Cutting speed	70-200 m/min		Cemented carbide: P20
Feed rate	0.05 mm/rev		Cermet (TiN)
Depth of cut	2 mm		Ceramics (Al_2O_3)
Lubricant	Dry		

point average roughness (Rz_{JIS}[2)]) was measured with a stylus type surface roughness tester after external turning under the conditions shown in **Table 3**. As tool materials, cemented carbide K10, cemented carbide P20, cermet (TiN) and a ceramic (Al_2O_3) were selected. The influence of tool wear on surface roughness was eliminated by using new tools at each test level. The external appearance of the tools after cutting was observed with a stereoscopic microscope. The rake face was then observed with a scanning electron microscope (SEM), and energy dispersive X-ray (EDX) analysis was performed. For comparison steel, S10C was used. Although S10C is inferior to SUM23 in terms of tool life, the as-rolled hardness is the same.

2.2 Experimental Results

Photo 1 shows the results of observation of the microstructure of the as-rolled steels. Although both SUM23 and S10C exibited microstructures consisting of pearlite dispersed in a ferrite matrix, pearlite bands parallel to the rolling direction were observed in SUM23. This feature is thought to occur because the Mn, P and S contents of SUM23 are higher than those of S10C, and as a result, the influence of microsegregation is strong. Regarding inclusions, a large number of coarse, fusiform (spindle-shaped) sulfides were dispersed in SUM23, whereas almost no coarse sulfides were observed in S10C. The hardness of both steels was substantially the same, being approximately 110 HV.

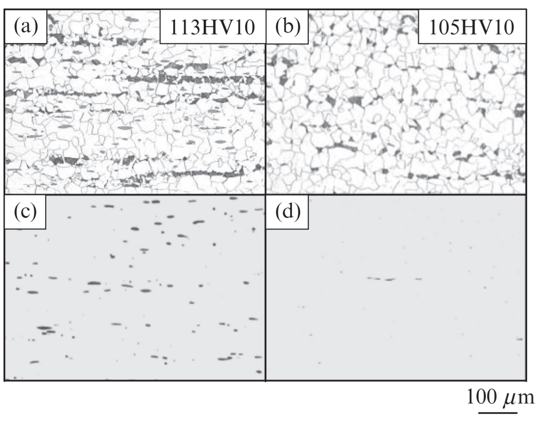

Photo 1 Optical micrographs of as-rolled steels
(a) SUM23 Microstructure (b) S10C Microstructure
(c) SUM23 Inclusions (d) S10C Inclusions

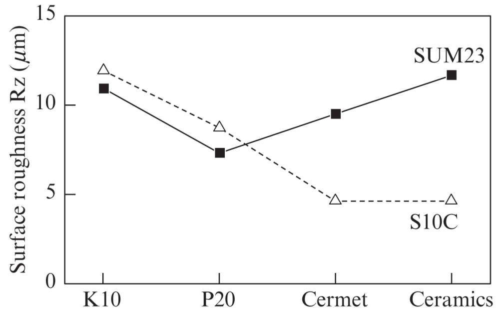

Fig. 1 Surface roughness after turning: Cutting speed at 70 m/min

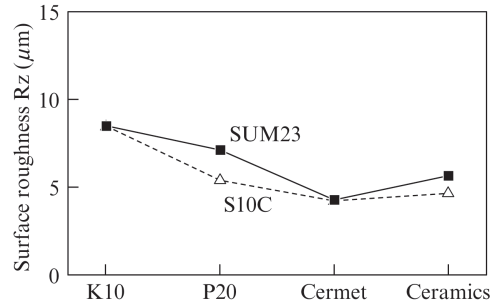

Fig. 2 Surface roughness after turning: Cutting speed at 100 m/min

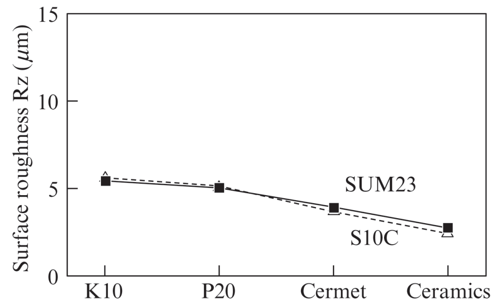

Fig. 3 Surface roughness after turning: Cutting speed at 200 m/min

Figure 1 shows the surface roughness after cutting with each tool at a cutting speed of 70 m/min[3)]. With SUM23, surface roughness increased pronouncedly with the cermet and ceramic tools in comparison with the two cemented carbide tools. At the cutting speed of 100 m/min in **Fig. 2**, the influence of the type of tool material on surface roughness was reduced, and when the speed was increased further and cutting was performed at 200 m/min (**Fig. 3**), the influence of the tool material showed a further decrease.

Photo 2 shows the external appearance of the cemented carbide K10 and ceramic tools after cutting

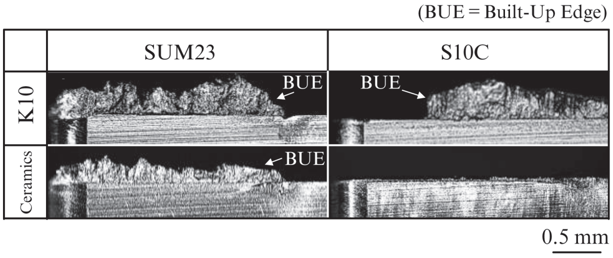

Photo 2 Tools after cutting: Cutting speed at 70 m/min

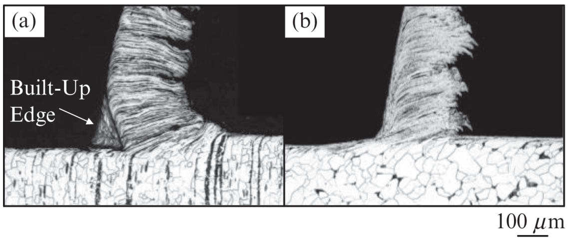

Photo 3 Chip formation behavior obtained by Quick Stop test (Tool: Ceramics) (a) SUM23 (b) S10C

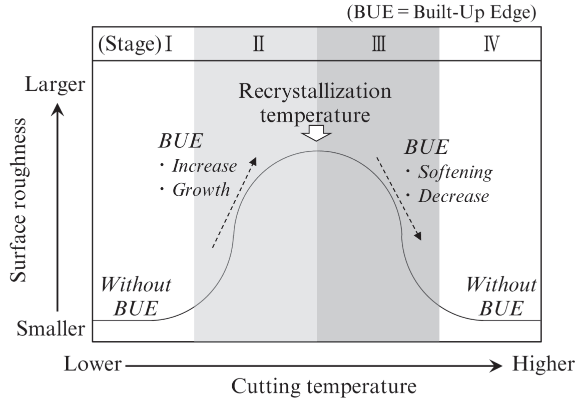

Fig. 4 Effect of Built-Up Edge and cutting temperature on surface roughness

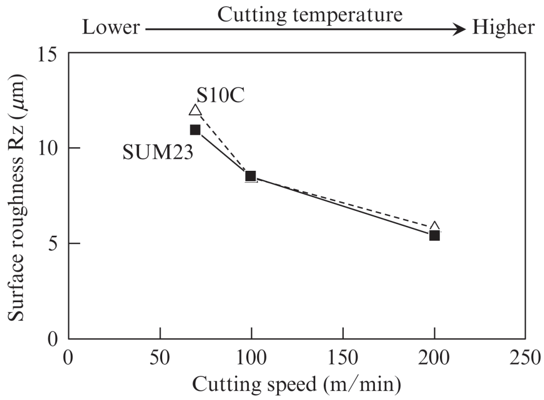

Fig. 5 Relationship between surface roughness and cutting speed with K10

at the speed of 70 m/min, that is, the speed at which the influence of the tool material was most remarkable[3]. In cutting with the cemented carbide K10, a built-up edge (BUE) was observed on the rake face with both SUM23 and S10C. On the other hand, with the ceramic tool, BUE was only observed with SUM23. **Photo 3** shows the results of observation of the condition of chips on the tool edge when a Quick Stop test was performed with the ceramic tool. From these results as well, BUE was also confirmed around the cutting point with SUM23, but was not observed with S10C. Based on the results described above, when cutting SUM23, it is estimated that BUE forms and falls off with high frequency, and as a result, surface roughness increases.

2.3 Discussion

It is thought that the type of tool material influences the surface roughness of SUM23 and S10C through the influence of BUE formation behavior. In general, the formation of BUE is considered to have a close relationship with the cutting temperature[4]. The influence of this relationship on the surface roughness is summarized in **Fig. 4**. It is thought that BUE does not occur until around 400°C (Stage I)[5]. At temperatures which are higher than 400°C but lower than the recrystallization temperature of the worked material (Stage II), formation and growth of BUE progress as the cutting temperature increases. On the other hand, at temperatures higher than the recrystallization temperature (Stage III), BUE softens and decreases as the cutting temperature rises, and at higher temperatures than this, BUE is no longer observed (Stage IV). It is considered that surface roughness is affected by this formation and extinction behavior of BUE, and shows an increasing tendency in Stage II and a decreasing tendency in Stage III in accordance with the cutting temperature. On the other hand, because BUE is not observed in Stage I and Stage IV, it is thought that surface roughness decreases in these stages, and the influence of the cutting temperature on surface roughness also becomes small.

The relationship between surface roughness and the cutting speed is shown in **Fig. 5** for cutting with the cemented carbide K10 tool and in **Fig. 6** for cutting with the ceramic tool. The cutting temperature is considered to have a positive correlation with the cutting speed. In the case of the cemented carbide K10 (Fig. 5), the surface roughness of both SUM23 and S10C decreases as the cutting speed increases. From this, it is thought that the cutting temperature is equivalent to Stage III with both SUM23 and S10C. In the case of the ceramic tool (Fig. 6), the surface roughness of SUM23 decreases accompanying increasing cutting speed, but with S10C, the decrease in surface roughness at higher cutting speeds is minimal because the surface roughness of this material was already small from the low cutting speed (70 m/min). From this, the cutting temperature of SUM23 is equivalent to Stage III, but

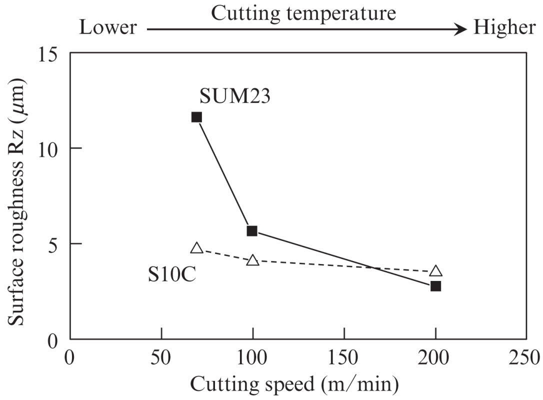

Fig. 6 Relationship between surface roughness and cutting speed with Ceramics

Table 4 Factors on cutting temperature

No.	Factors
1	Cooling by lubricant
2	Thermal conductivity of worked material
3	Thermal conductivity of tool material
4	Cutting resistance

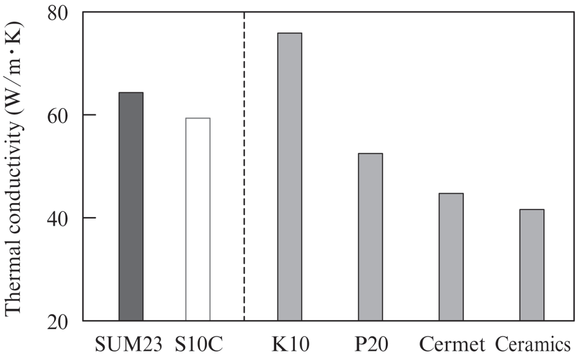

Fig. 7 Comparison of thermal conductivity

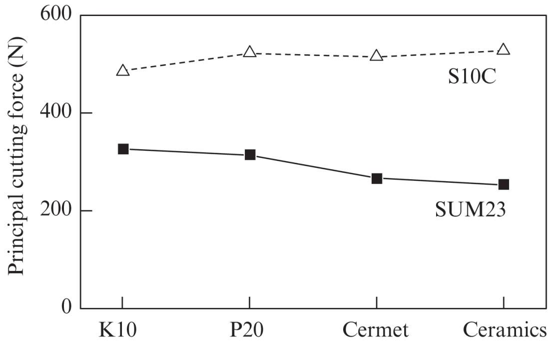

Fig. 8 Cutting resistance: Cutting speed at 70 m/min

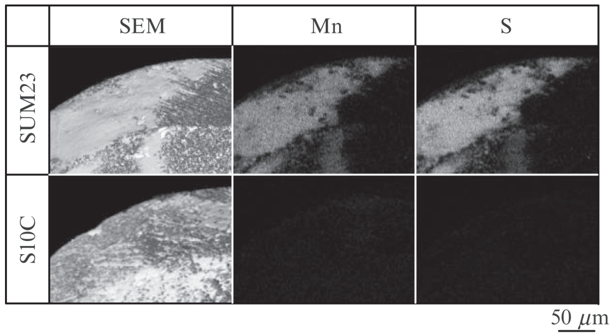

Photo 4 Analysis on rake face after cutting (Tool: Ceramics, speed at 70 m/min)

with S10C, it can be thought that the cutting temperature is equivalent to the higher temperature Stage IV.

The factors which influence the cutting temperature are arranged in **Table 4**. **Figure 7** shows the thermal conductivity (catalogue values) of the worked materials[6)] and tool materials. The thermal conductivity of S10C is smaller than that of SUM23, and among the tool materials, the thermal conductivity of the ceramic is the smallest. From this, it can be said that S10C shows a heat accumulation tendency in comparison with SUM23, and the ceramic material shows a heat accumulation tendency in comparison with the cemented carbides. **Figure 8** shows the influence of the tool material on cutting resistance (principal cutting force) at the speed of 70 m/min with SUM23 and S10C. In spite of the fact that the hardness of the two steels is the same, the cutting resistance of S10C is approximately 2 times larger than that of SUM23. Based on this, heat generation during cutting is larger with S10C than with SUM23. Therefore, when cutting S10C with the ceramic tool, both of which tend to accumulate heat, the cutting condition is high temperature cutting in Stage IV, even at the low cutting speed (70 m/min).

The main factor in the cutting resistance of SUM23 is considered to be the effect of sulfides in promoting initiation and propagation of microcracks. **Photo 4** shows examples of the results of SEM observation of the tool rake face after cutting and EDX analysis of the distributions of Mn and S. After cutting SUM23, formation of a sulfide (MnS) film was observed on the tool rake face. That is, in addition to the above-mentioned effect of promoting initiation/propagation of microcracks, sulfides also form a film which increases the lubricity between the tool and the worked material, and it is possible that this contributed to the large decrease in the cutting resistance of SUM23.

3. Influence of Sulfide Formation and Yield Ratio on Surface Roughness

3.1 Experimental Method

SUM23 (0.08 C-1.2 Mn-0.06 P-0.35 S) was used as the test steel. A 150 kg ingot was melted with a vacuum melting furnace and breakdown rolling was performed to a thickness of 100 mm. In order to vary the sulfide morphology and yield ratio (ferrite grain diameter),

Table 5 Turning test conditions

Tool shape	TNGN160404	Lubricant	Dry Wet
Cutting speed	70 m/min		
Feed rate	0.02 mm/rev	Tool material	Cemented carbide P20 Ceramics (Al_2O_3)
Depth of cut	1 mm		

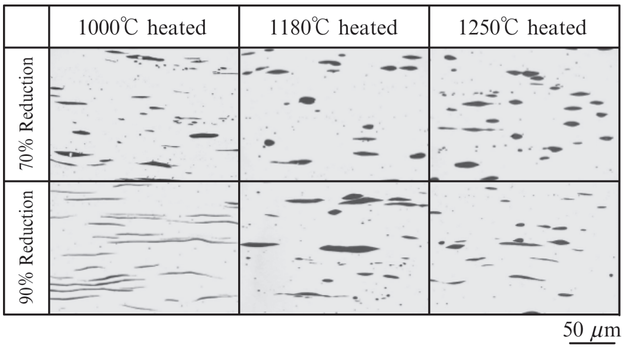

Photo 5 Sulfides in as-rolled SUM23

this material was reheated to various temperatures, and then rolled to a cumulative reduction of 70% (thickness: 30 mm) or 90% (thickness: 10 mm). Round bars with a diameter of 9.5 mm were then cut from the obtained plates, and sulfides were observed at a depth of 1 mm from the surface. Using image analysis, the size of the sulfides was evaluated by the equivalent circle diameter and the aspect ratio was evaluated by the length/width ratio.

The sulfide size was obtained by the equivalent circle diameter and the aspect ratio was obtained by image analysis of the length/width ratio. For roughness, after external turning of round bars with a diameter of 9.5 mm under the conditions shown in **Table 5**, Rz_{JIS} was measured with a stylus type surface roughness tester.

The yield ratio was obtained by a tensile test using JIS No. 4 test pieces cut from the as-rolled steel.

3.2 Experimental Results

Photo 5 shows the results of observation of the sulfides in the as-rolled steel, and **Fig. 9** shows the result when the sulfide size and aspect ratio were arranged by the heating temperature. The sulfide size showed constant values independent of the heating temperature and cumulative reduction. On the other hand, the sulfide aspect ratio showed a constant value independent of the heating temperature under cumulative reduction of 70%, but under the combined conditions of 90% cumulative reduction and low temperature (1 000°C) heating, the aspect ratio increased pronouncedly, that is, the sulfides were elongated. **Figure 10** shows the relationship between the yield ratio and the heating temperature. The yield ratio was increased by high cumulative reduction and low temperature heating.

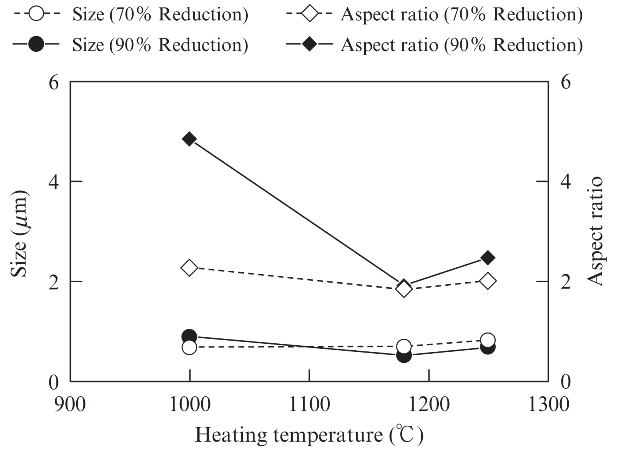

Fig. 9 Effect of heating temperature on size and aspect ratio of sulfides

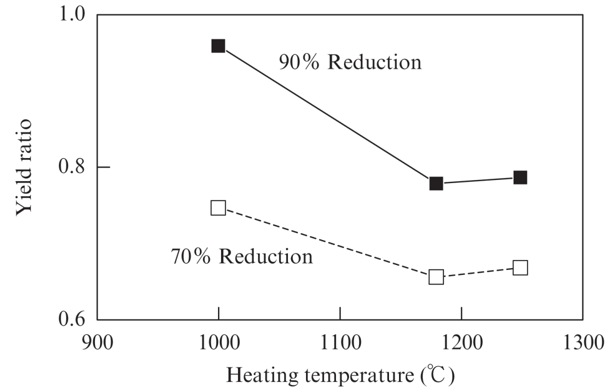

Fig. 10 Effect of heating temperature on yield ratio

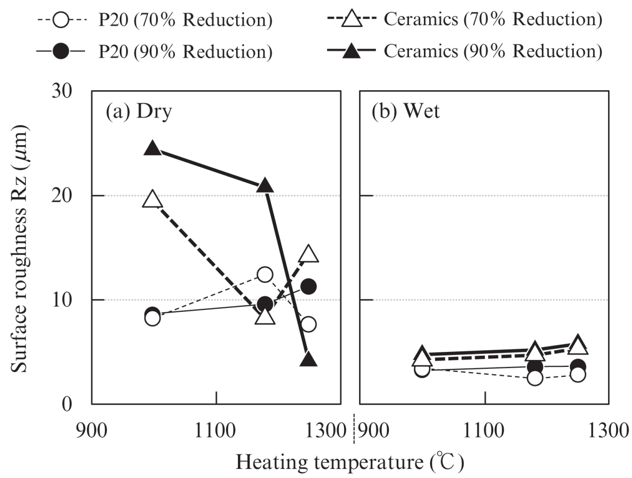

Fig. 11 Surface roughness after turning (a) Dry (b) Wet

Figure 11 (a) and (b) show the surface roughness after dry turning and wet turning, respectively[7]. With dry turning, surface roughness showed diverse changes under the various conditions. This was considered to be the result of diverse changes in the formation of BUE due to the influence of the various factors on the cutting temperature. In comparison with dry turning, surface roughness was generally lower with wet turn-

Table 6 Results of multiple regression analysis

Tool material	Lubricant	Multiple regression equation	Order of $\|t\|$
P20	Dry	$Rz = 50.3 - 47.6YR - 22.0\alpha + 3.9\beta$	$\alpha > \beta > YR$
Ceramics	Dry	$Rz = 36.1 - 4.8YR - 45.0\alpha + 6.5\beta$	$\alpha > \beta > YR$
P20	Wet	$Rz = 10.4 - 4.9YR - 7.8\alpha + 0.9\beta$	$\alpha > \beta > YR$
Ceramics	Wet	$Rz = 36.8 - 32.2YR - 22.7\alpha + 3.4\beta$	$\alpha > \beta > YR$

YR: Yield ratio
α: Size of sulfides
β: Aspect ratio of sulfides
$|t|$: Absolute value of t ratio

ing. It is estimated that this behavior occurred because the cutting temperature decreased pronoucedly under all of these conditions due to the cooling effect of the lubricant, and as a result, the cutting temperature was in the Stage I region.

3.3 Influence of Sulfide Morphology and Yield Ratio

Table 6 shows the results of a multiple regression analysis which was performed to determine the degree of influence of the sulfide morphology and yield ratio on surface roughness. The table also shows the order of $|t|$, which is an index showing the degree of influence of the factors. With both the cemented carbide tool and the ceramic tool, the order of $|t|$ was Size of sulfides > Aspect ratio of sulfides > Yield ratio, regardless of whether a lubricant was used or not. Thus, within the range of this study, it can be thought that the influence of the tool material on the order of the influence of the steel-related factors is small. Furthermore, focusing on the signs of the coefficients of each factor, this study has shown that increasing the sulfide size, decreasing the sulfide aspect ratio (fusiform sulfides) and increasing the yield ratio (refinement of ferrite) are effective for reducing surface roughness.

4. Conclusion

In this study, the influence of the type of tool material and the influence of steel-related factors on the surface roughness after cutting low carbon resulfurized free cutting steel were clarified. However, as shown in Table 1, the influence factors on the surface roughness are numerous, and taking into consideration the combination, it is still far from understanding the whole picture. In addition to the surface roughness, tool life and chip handling properties can not be neglected as machinability. In order to respond to these challenges and improve the machinability of low carbon resulfurized free cutting steel, a deeper fundamental understanding of cutting phenomena is necessary. For this, in-*situ* monitoring of the cutting temperature and chips is considered an essential task.

References

1) Shiraga, T. CAMP-ISIJ. 1999, vol. 12, p. 961.
2) JIS B 0601. Geometrical Product Specifications (GPS)-Surface texture. 2013.
3) Murakami, T.; Tomita, K.; Shiraga, T. CAMP-ISIJ. 2008, vol. 21, p. 1227.
4) Ito, T.; Abeyama, S.; Nakamura, S. Previous printing of spring lecture conference of The Japan Society for Precision Engineering. 1976, p. 137.
5) Abeyama, S.; Nakamura, S. Machinability Testing and Utilization of Machining Data. 1979, ASM, p. 184.
6) Japan Society for the Promotion of Science and The Iron and Steel Institute of Japan. Tekkonetsukeisanyosuchi. 1966.
7) Shiraga, T.; Murakami, T.; Tomita, K. CAMP-ISIJ. 2010, vol. 23, p. 1057.